

Rigorous Interpretation of Electronic Density Functions of Axial and Equatorial Conformers of Dimethylphosphinoylcyclohexane, 2-(Dimethylphosphinoyl)-1,3,5-trithiane, and 2-(Dimethylphosphinoyl)-1,3-dithiane-1,1,3,3-tetraoxide

Gustavo Madrid,[†] Ana Rochín,[‡] Eusebio Juaristi,^{*,#} and Gabriel Cuevas^{*,†}

Instituto de Química, Universidad Nacional Autónoma de México, Circuito Exterior, Ciudad Universitaria, Coyoacán 04510, México, D.F., Mexico, Escuela de Ciencias Químicas, Universidad La Salle, Benjamín Franklin 47, Hipódromo Condesa, 06140 México, D.F., Mexico, and Departamento de Química, Centro de Investigación y de Estudios Avanzados del Instituto Politécnico Nacional, Apdo. Postal 14-740, 07000 México, D.F., Mexico

gecgb@servidor.unam.mx

Received October 23, 2000

Theoretical analysis within the frame of the Topological Theory of Atoms in Molecules confirms the repulsive steric interaction between an axial dimethylphosphinoyl group and the *syn*-diaxial hydrogens in cyclohexane derivative **2-ax**. In seemingly good agreement with experiment, equatorial isomer **2-eq** was calculated to be 1.49 kcal/mol more stable than **2-ax**. (Experimental energy difference in (diphenylphosphinoyl)cyclohexane, $\Delta H^\circ = 1.96$ kcal/mol.) In contrast, *axial* 2-(dimethylphosphinoyl)-1,3,5-trithiane, **3-ax**, was calculated to be 6.38 kcal/mol more stable than **3-eq**. (Experimentally, the axial conformer of 2-(diphenylphosphinoyl)-1,3,5-trithiane, was found to be 1.43 kcal/mol more stable than the equatorial conformer, in solvent chloroform.) Theoretical analysis, in particular the electron density at the bond critical point within the C(4,6)-H \cdots O=P bonding trajectory, implies significant bonding in this segment of interacting atoms. By the same token, substantial positive charge is acquired by the C–H bonds adjacent to the sulfonyl groups in disulfone **4**. Hydrogen bonding between the phosphoryl group and H(4,6) leads to stabilization of **4-ax**, which is estimated to be 5.0 kcal/mol lower in energy than **4-eq**. This conclusion is supported by examination of P=O \cdots H–C(4,6) bond trajectories, as well as from evaluation of the critical point properties along those interacting moieties. By contrast, fluorinated derivative **5** is more stable in the equatorial conformation, indicating a repulsive electrostatic interaction of the C–F \cdots O–P entity in **5-ax**.

Introduction

In 1982 Juaristi and co-workers^{1a} reported the predominance of the axial conformation of 2-(diphenylphosphinoyl)-1,3-dithiane (**1-ax**, Figure 1), and subsequent studies^{1b,c} demonstrated that the S–C–P anomeric effect operative in this system is worth ca. 3.0 kcal mol^{–1}, one of the largest yet recorded.

The origin of the anomeric effect in **1-ax** has proved controversial since X-ray structural data^{1d} do not reproduce the bond length deformations anticipated from $n_S \rightarrow \sigma^*_{C-P}$ stereoelectronic interactions; i.e., neither shortening of the S–C(2) bonds nor lengthening of the C(2)–P bond was observed.^{1d} In this regard, the phosphoryl group in **1-ax** is forced into close proximity with the *syn*-diaxial hydrogens [P–O \cdots H(4,6-ax) = 2.46 Å^{1d}] so that Coulombic attraction between a partially negative phosphoryl

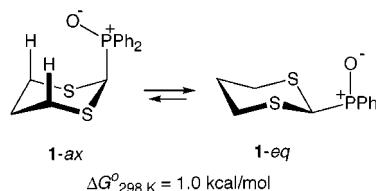


Figure 1. Conformational preference of 2-diphenylphosphino-1,3-dithiane (**1**).

oxygen and slightly positively charged H(4,6-ax) became an attractive complementary/alternative rationalization of the experimental findings.^{1b,c,e,2} Nevertheless, substantial data,^{1c} including a very recent microwave analysis,^{2c} are not in line with this argument.

Recently,^{2d} the C–H \cdots O=P bond trajectories in 2-(dimethylphosphinoyl)-1,3-dithiane were described, as well as the properties of the critical points associated with them. The characterization of these bond paths is relevant because it allows one to establish that interactions of the hydrogen-bond type can make a stabilizing contribution

* To whom correspondence should be addressed.

[†] Instituto de Química. UNAM. Contribution No. 1729.

[‡] Escuelas de Ciencias Químicas. ULSA.

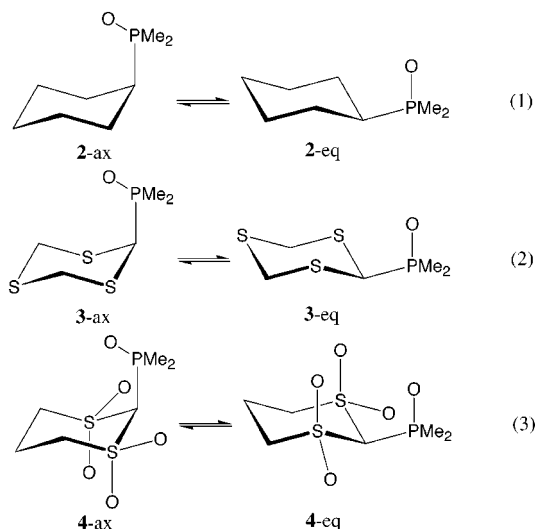
[#] Centro de Investigación y de Estudios Avanzados del Instituto Politécnico Nacional.

(1) (a) Juaristi, E.; Valle, L.; Mora-Uzeta, C.; Valenzuela, B. A.; Joseph-Nathan, P.; Fredrich, M. F. *J. Org. Chem.* **1982**, *47*, 5038. (b) Juaristi, E.; Valle, L.; Valenzuela, B. A.; Aguilar, M. A. *J. Am. Chem. Soc.* **1986**, *108*, 2000. (c) Juaristi, E.; Cuevas, G. *The Anomeric Effect*; CRC Press: Boca Raton, FL, 1995; Section 7.3. (d) Juaristi, E.; Valenzuela, B. A.; Valle, L.; McPhail, A. T. *J. Org. Chem.* **1984**, *49*, 3026. (e) Valle, L. Masters Thesis, Cinvestav-IPN, México, 1982.

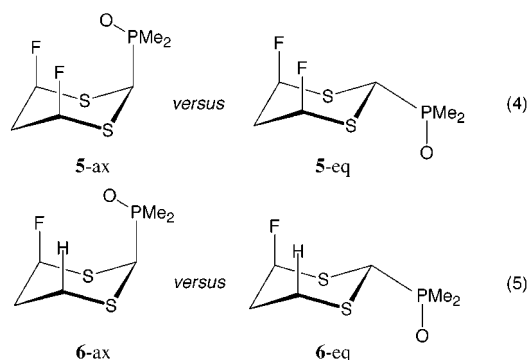
(2) (a) Mikolajczyk, M.; Bolczewski, P.; Wroblewski, K.; Karolak-Wojciechowska, J.; Miller, A.; Wieczorek, M. W.; Antipin, M. Y.; Struchkov, Y. T. *Tetrahedron*, **1984**, *40*, 4885. (b) Mikolajczyk, M.; Graczyk, P.; Wieczorek, M. W. *J. Org. Chem.*, **1994**, *59*, 1672. (c) Graczyk, P. P.; Mikolajczyk, M.; Plass, M.; Kolbe, A. *J. Mol. Struct.* **1997**, *416*, 179. (d) Cuevas, G. *J. Am. Chem. Soc.* **2000**, *122*, 692.

to the axial conformational preference of the S–C–P(O) anomeric segment.

In this paper, the conformational equilibria of the dimethylphosphinoyl group were studied in cyclohexane (2), 1,3,5-trithiane (3), and 1,1,3,3-tetraoxa-1,3-dithiane (4). Disulfone derivative 4 was deemed an attractive subject for study since the lack of sulfur lone pairs precludes $n_S \rightarrow \sigma^*_{C-P}$ hyperconjugation, whereas the sulfonyl group confers significant acidity to the adjacent methylene hydrogens.³ (eqs 1–3).



To gain additional information regarding the nature of the C–H···O=P interaction, the axial hydrogen atoms at C(4,6) were substituted by fluorine atoms (eq 4). The repulsive nature of the C–F···O=P interaction in 5-ax is manifest. In the monofluoride derivative 6, the phosphoryl oxygen of the axial conformer points toward the remaining *syn*-diaxial hydrogen atom H(6-ax) (eq 5).



Computational Methods

Full geometry optimization of all compounds studied here were performed at B3LYP/6-31G(*d,p*) level, and from the G94 program⁴ wave function archive, the AIMPAC⁵ set of programs were used, obtaining the properties of atoms and critical points (cps) in the charge density: density (ρ), Laplacians ($\nabla^2\rho$), and ellipticities (ϵ).

Two of the most important contributions of the AIM theory are the following: the precise definition of an atom in a molecule and the definition of the chemical bond. These concepts correspond to the topological properties of the electron

density.^{6–8} The chemical structure of a molecule is unambiguously described determining the critical points through the electron density and corresponds to the gradient zero density points. These points, as well as the first and second derivatives, can be determined with the use of the PROAIM⁵ program. From the second derivative, it is possible to determine the three principal curvatures associated with a critical point due to its index (the algebraic addition of the curvature sign).

A negative curvature implies that the density (ρ) is in a maximum at that point. ρ 's gradient is a vector directed toward ρ increase. If a succession of points is calculated in which each new point is determined by the previous point, a high charge density path is obtained. This path normally ends in a nucleus, but if there is a nucleus close to the first one, there is necessarily a demarcation surface between them, and the paths are forced to end in a critical point (3, –1). This means that there has to be a surface where $\rho(r)$ is a maximum in a critical point, with two negative curvatures. The positive curvature of this critical point is associated with the axis, perpendicular to the interatomic surface, in which $\rho(r)$ is a minimum. This axis defines the initial direction of two $\nabla\rho$ paths that originate in this critical point and end in the nucleus. This line of maximal density with respect to the gradient paths is called the bonding path. According to Bader,^{7,9} "the existence of a bonding path is a necessary condition and is enough for the existence of a bond".

The presence of a bond path and its associated virial path provides a universal indicator of bonding between the atoms so linked. Since weak interactions are primarily the result of a correlation of the electron motions on the two interacting species, their description requires the use of densities obtained from correlated wave functions, determined in an exact manner by DFT methods.

Besides density, ellipticity is an important property of a critical point. This is defined as the coefficient of the negative curves along the perpendicular axis to the bonding path: $\epsilon = \lambda(1)/\lambda(2) - 1$ and should be considered as an index of bond's anisotropy. If the studied bond belongs to a ring or a cage, two or more of its interatomic surfaces will have critical points (3, +1), called ring critical points and (3, +3), which is a cage critical point. The Poincaré–Hopf relation determines the type of critical points that can coexist in a system. For a number of n nucleus associated with b bond paths, r rings, and c cages, the relation establishes

$$n - b + r - c = 1$$

The numbers n , b , r , and c are the characteristic set for the molecule.^{9a} The characterization of the critical points allows one to establish the molecular structure, as well as to study the chemical bonds in unusual conditions because the topological approximation does not show a difference between a normal (strong) bond and those resulting from weak interactions.^{9,10}

(4) Frisch, M. J.; Trucks, G. W.; Schlegel, H. B.; Gill, P. M. W.; Johnson, B. G.; Robb, M. A.; Cheeseman, J. R.; Keith, T.; Petersson, G. A.; Montgomery, J. A.; Raghavachari, K.; Al-Laham, M. A.; Zakrzewski, V. G.; Ortiz, J. V.; Foresman, J. B.; Cioslowski, J.; Stefanov, B. B.; Nanayakkara, A.; Challacombe, M.; Peng, C. Y.; Ayala, P. Y.; Chen, W.; Wong, M. W.; Andres, J. L.; Replogle, E. S.; Gomperts, R.; Martin, R. L.; Fox, D. J.; Binkley, J. S.; Defrees, D. J.; Baker, J.; Stewart, J. P.; Head-Gordon, M.; Gonzalez, C.; Pople, J. A. *Gaussian 94*, revision D.4; Gaussian, Inc.: Pittsburgh, PA, 1995.

(5) Beigler-Köming, F. W.; Bader, R. F. W.; Tang T. H. *J. Comput. Chem.* **1982**, 3, 317.

(6) Bader, R. F. W.; Carroll, M. T.; Cheeseman, J. R.; Chang, C. J. *Am. Chem. Soc.* **1987**, 109, 7968.

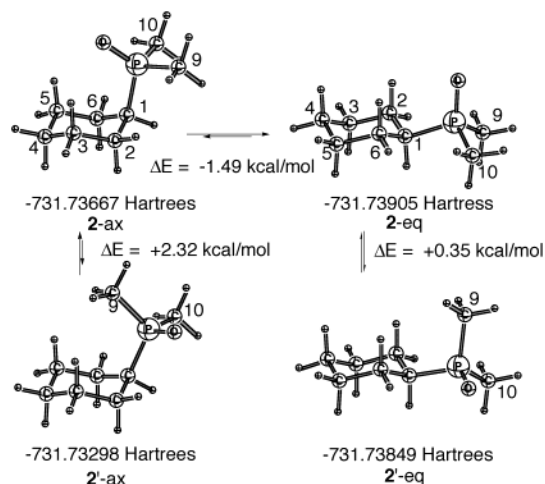
(7) Bader, R. F. W.; Essen, H. *J. Chem. Phys.* **1984**, 80, 1943.

(8) Bader, R. F. W. *J. Phys. Chem. A* **1998**, 102, 7314.

(9) (a) Bader, R. F. W. *Atoms in Molecules, a Quantum Theory*; Clarendon Press: Oxford, 1990. (b) Bader, R. F. W. *Chem. Rev.* **1991**, 91, 893. (c) Bader, R. F. W. *Acc. Chem. Res.* **1985**, 18, 9. (d) Bader, R. F. W. *Chem. Rev.* **1991**, 91, 893.

(10) (a) Cioslowski, J.; Mixon, S. T.; Edwards, W. D. *J. Am. Chem. Soc.* **1991**, 113, 1083. (b) Cioslowski, J. *J. Am. Chem. Soc.* **1993**, 115, 5177. (c) Cioslowski, J. *J. Phys. Chem.* **1990**, 94, 5496.

(3) (a) Streitwieser, A., Jr.; Juaristi, E.; Nebenzahl, L. L. In *Comprehensive Carbanion Chemistry*; Buncl, E., Durst, T., Eds.; Elsevier: Amsterdam, 1980; Chapter 7. (b) Bordwell, F. G. *Acc. Chem. Res.* **1988**, 21, 456.

Scheme 1. Conformational Equilibria of 1-(Dimethylphosphinoyl)-cyclohexane^a^a ZPE corrections are not included.

Results and Discussion

Complete geometry optimizations (without symmetry constraints) of all compounds and related conformers studied here were carried out within the frame of DFT at the Becke3LYP/6-31G(*d,p*) level with the Gaussian 94 program (G94).⁴ Low energy isomers maintain a chair conformation in all compounds.

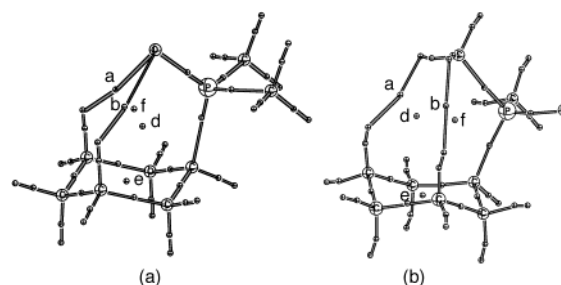
Part A. Conformational Analysis of 2-(Dimethylphosphinoyl)cyclohexane. 2. We first examined cyclohexyl derivative **2**. Scheme 1 summarizes the energetics of its conformational behavior, and Table 1 lists the structural features of the relevant conformers of minimum energy. The most stable conformer is **2-eq**, which is calculated to be 1.49 kcal/mol lower in energy than **2-ax**. This seems to be in good agreement with the experimental result $\Delta H_{\text{ax/eq}} = -1.96$ kcal/mol, for (diphenylphosphinoyl)cyclohexane in solvent chloroform.¹¹

Interestingly, **2-ax** (phosphoryl-inside rotamer) is estimated to be substantially lower in energy relative to **2'-ax** (methyl inside rotamer). By contrast, equatorial rotamers **2-eq** and **2'-eq** are almost isoenergetic, $\Delta E = +0.35$ kcal/mol. These observations are in line with the experimental finding of a significant entropy gain in going from axial to equatorial (diphenylphosphinoyl)-cyclohexane—the axial group being conformationally constrained to rotamers with the P–O bond above the cyclohexane ring, whereas an equatorial diphenylphosphinoyl is more free to fully rotate around the C–P bond.¹¹

The substantially lower energy of **2-eq** relative to **2-ax** is readily ascribed to steric repulsion between the axial substituent and the methylenes at C(3,5).¹² Indeed, topological analysis of conformer **2-ax** was possible by means of AIMPAC⁵ (Atoms in Molecules Package), a set of programs that defines the properties of atoms and bonding patterns [charge density (ρ), Laplacians ($\nabla^2\rho$),

Table 1. Geometry of Relevant Conformers of (Dimethylphosphinoyl)-cyclohexane (2**) at the B3LYP/6-31G(*d,p*) Level (Distances in Å, Angles in Degrees)^a**

	2-ax	2'-ax	2-eq	2'-eq
C ₁ –C ₂	1.549	1.547	1.545	1.542
C ₂ –C ₃	1.538	1.535	1.537	1.539
C ₃ –C ₄	1.536	1.535	1.534	1.536
C ₄ –C ₅	1.536	1.535	1.534	1.536
C ₅ –C ₆	1.538	1.539	1.537	1.536
C ₆ –C ₁	1.549	1.548	1.545	1.544
C ₁ –P	1.858	1.864	1.853	1.853
P–O	1.507	1.505	1.505	1.504
P–C ₉	1.838	1.837	1.836	1.836
P–C ₁₀	1.838	1.837	1.836	1.835
C ₁ –C ₂ –C ₃	113.0	113.5	111.9	111.1
C ₂ –C ₃ –C ₄	111.3	111.4	111.7	111.8
C ₃ –C ₄ –C ₅	111.2	111.1	111.0	111.4
C ₄ –C ₅ –C ₆	111.3	111.9	111.7	111.7
C ₅ –C ₆ –C ₁	113.0	114.4	111.9	111.3
C ₆ –C ₁ –C ₂	110.0	111.9	110.6	111.0
C ₂ –C ₁ –P	112.8	111.9	110.7	116.0
C ₆ –C ₁ –P	112.8	117.6	110.7	110.5
C ₁ –P–O	115.8	111.9	113.9	112.6
C ₁ –P–C ₉	104.9	111.0	105.4	106.9
C ₁ –P–C ₁₀	104.9	103.6	105.4	105.4
C ₁ –C ₂ –C ₃ –C ₄	54.8	54.0	55.0	55.2
C ₂ –C ₃ –C ₄ –C ₅	55.5	56.9	55.0	54.5
C ₃ –C ₄ –C ₅ –C ₆	55.5	55.1	55.0	54.4
C ₄ –C ₅ –C ₆ –C ₁	54.8	50.6	55.0	55.0
C ₅ –C ₆ –C ₁ –C ₂	52.6	46.5	53.9	55.5
C ₆ –C ₁ –C ₂ –C ₃	52.6	48.1	53.9	55.5
C ₂ –C ₁ –P–O	62.7	36.5	61.5	176.2
C ₆ –C ₁ –P–O	62.7	168.0	61.5	48.8
C ₃ –C ₂ –C ₁ –P	74.3	86.2	177.0	177.3
C ₅ –C ₆ –C ₁ –P	74.3	85.0	177.0	174.4
C ₂ –C ₁ –P–C ₉	63.2	90.8	64.1	50.8
C ₂ –C ₁ –P–C ₁₀	171.4	159.4	172.9	59.5

^a See Scheme 1 for system numbering.**Figure 2.** Critical points in the electron density of (a) **2-ax** and **2'-ax**, calculated at the Becke3LYP/6-31G(*d,p*) level of theory.

and ellipticities (ϵ) of critical points between atoms] in a molecule.⁹ Most relevant, the bond trajectories C(3,5)–H_{ax}–O–P present low electronic density at the critical points *a* and *b* (0.009 e/a_0^3 , respectively; Figure 2a and Table 2).¹³

Population analysis of **2-ax** indicates a slightly positive charge (+0.1 e) at the *syn*-diaxial C–H hydrogens, which should originate an attractive electrostatic interaction with the negatively charged phosphoryl oxygen (–1.10 e). It is thus clear that another effect makes the net interaction repulsive in axial dimethylphosphinoylcyclohexane. The simplest explanation can be deduced from the geometry parameters of the cyclohexane ring (relatively short C–C bonds), which results in overriding

(11) Juaristi, E.; Lopez-Nuñez, N. A.; Glass, R. S.; Petsom, A.; Hutchins, R. O.; Stercho, J. P. *J. Org. Chem.* **1986**, *51*, 1357.

(12) Juaristi, E. *Introduction to Stereochemistry and Conformational Analysis*; Wiley: New York, 1991. (b) Eliel, E. L.; Wilen, S. H.; Mander, L. N. *Stereochemistry of Organic Compounds*; Wiley: New York, 1994. (c) *Conformational Behavior of Six-Membered Rings: Analysis, Dynamics, and Stereoelectronic Effects*; Juaristi, E., Ed.; VCH Publishers: New York, 1995.

(13) By contrast, bonding interactions are usually associated with much larger electronic densities; for example, a typical A–H–B hydrogen bond presents $r \geq 0.36$ $e/\text{\AA}^3$.⁹

Table 2. Properties of Critical Points Associated to Weak Interactions in Compounds 2-ax-4-ax

point ^a	ρ (e/a ₀ ³)	$\nabla^2\rho$	ϵ	x^b	y^b	z^b	TBP ^c	GD ^d
2-ax/a	0.009	0.031	0.171	-0.008	-0.007	0.050	4.968	4.899
2-ax/b	0.009	0.031	0.171	-0.008	-0.007	0.050	4.967	4.898
2-ax/d	0.007	0.033		-0.005	0.008	0.030		
2-ax/e	0.017	0.109		-0.014	0.059	0.064		
2-ax/f	0.007	0.033		-0.005	0.008	0.030		
2'-ax/a	0.005	0.020	0.469	-0.004	-0.003	0.028	5.383	4.320
2'-ax/b	0.003	0.012	0.074	-0.003	-0.003	0.018	4.578	4.564
2'-ax/d	0.002	0.010		-0.001	0.004	0.007		
2'-ax/e	0.017	0.075		-0.013	0.038	0.052		
2'-ax/f	0.004	0.015		-0.002	0.005	0.011		
2-eq/a	0.017	0.110		-0.014	0.060	0.064		
3-ax/a	0.012	0.039	0.061	-0.011	-0.011	0.061	4.60	4.55
3-ax/b	0.012	0.039	0.061	-0.011	-0.011	0.061	4.60	4.55
3-ax/c	0.005	0.023		-0.003	0.011	0.014		
3-ax/d	0.007	0.035		-0.004	0.012	0.027		
3-ax/e	0.010	0.054		-0.004	0.028	0.030		
3-ax/f	0.007	0.035		-0.004	0.012	0.027		
3-ax/g	0.005	0.022		0.004	0.008	0.010		
3-eq/a	0.011	0.055		-0.005	0.030	0.030		
4-ax/a	0.011	0.036	0.049	-0.011	-0.010	0.057	4.69	4.63
4-ax/b	0.011	0.036	0.049	-0.011	-0.010	0.057	1.69	4.63
4-ax/c	0.0056	0.024		-0.03	0.013	0.013		
4-ax/d	0.0069	0.032		-0.04	0.012	0.024		
4-ax/e	0.011	0.63		-0.006	0.035	0.035		
4-ax/f	0.0069	0.032		-0.004	0.012	0.024		
4-ax/g	0.0051	0.022		0.005	0.006	0.011		
4-ax/h	0.015	0.054	0.146	-0.016	-0.014	0.083	4.43	4.31
4-ax/i	0.015	0.054	0.151	-0.015	-0.013	0.083	4.433	4.31
4-ax/j	0.0092	0.040		-0.006	0.009	0.036		
4-ax/k	0.0092	0.040		-0.006	0.009	0.036		
4-ax/l	0.0094	0.031	0.50	-0.007	-0.005	0.042	5.72	5.69
4-ax/m	0.004	0.037		-0.006	0.006	0.037		
4-ax/n	0.280	1.003	0.055	-0.457	-0.434	1.894	2.78	2.78
4-ax/o	0.283	1.061	0.047	-0.459	-0.438	1.959	2.77	2.77
4-ax/p	0.280	1.003	0.055	-0.457	-0.434	1.894	2.78	2.78
4-ax/q	0.283	1.061	0.047	-0.459	-0.438	1.959	2.77	2.77

^a See Figures for numbering. ^b Eigenvalues of the Hessian at critical points. ^c Total bond path (au). ^d Geometric distance (au).

steric repulsion between the phosphoryl group and the axial hydrogens. Supporting data for this interpretation comes from calculated structural data, e.g., C–C–P bond angles in 2-ax are ca. 112.8° versus 110.7° in 2-eq, and C–P–O bond angles in 2-ax are in average 115.8° versus 112.9° in 2'-eq. Similarly, the average C–C–C–P dihedral angle is a significant 74.3°, to be compared with an ideal 60° for an undistorted chair conformation.

Topological analysis of rotamer 2'-ax was deemed of interest in view of the anticipated increased steric repulsion between the *P*-methyl group and the ring hydrogens (Figure 2b and Table 2). Again, the properties of the critical points *a* and *b*—in particular the very low electron densities (0.005 and 0.003 e/a₀³, respectively)—are characteristic of nonbonding steric interactions between atoms in close proximity.¹⁰

Part B. Conformational Analysis of 2-(Dimethylphosphinoyl)-1,3,5-trithiane, 3. Table 3 presents the calculated geometries for the most relevant (lower energy) conformers in axial and equatorial 2-(dimethylphosphinoyl)-1,3,5-trithiane. Rotamer 3-ax is estimated to be 5.0 kcal/mol more stable than 3'-eq, the equatorial rotamer of lower energy (Scheme 2).

Although agreement with the experimentally observed results [$\Delta G_{ax/eq}^\circ = -1.49$ kcal/mol for 2-(diphenylphosphinoyl)-1,3,5-trithiane in solvent chloroform^{1b}] is not as good, the ab initio calculation does reproduce the observed axial preference of the phosphorus substituent.

It is of relevance to compare the relative energies of 2-ax and 2'-ax ($\Delta E = +2.32$ kcal/mol, Scheme 1) with

Table 3. Geometry of Most Relevant Conformers of 2-(Dimethylphosphinoyl)-1,3,5-Trithiane (3) at the B3LYP/6-31G(d,p) Level (Distances in Å, Angles in Degrees)^a

	3-ax	3'-ax	3-eq	3'-eq
S ₁ –C ₂	1.843	1.846	1.840	1.843
C ₂ –S ₃	1.843	1.838	1.840	1.840
S ₃ –C ₄	1.840	1.828	1.833	1.830
C ₄ –C ₅	1.827	1.829	1.829	1.830
C ₅ –C ₆	1.827	1.825	1.830	1.826
C ₆ –S ₁	1.840	1.834	1.833	1.834
C ₂ –P	1.870	1.885	1.877	1.880
P–O	1.507	1.499	1.497	1.498
P–C ₉	1.830	1.832	1.830	1.827
P–C ₁₀	1.830	1.832	1.831	1.829
S ₁ –C ₂ –S ₃	115.4	116.4	114.3	115.2
C ₂ –S ₃ –C ₄	101.1	103.3	98.1	99.3
S ₃ –C ₄ –C ₅	115.7	116.6	116.7	117.2
C ₄ –C ₅ –C ₆	97.8	97.3	98.9	98.2
C ₅ –C ₆ –S ₁	115.7	116.9	116.5	116.5
C ₆ –S ₁ –C ₂	101.1	103.7	98.1	99.7
S ₁ –C ₂ –P	112.3	117.0	109.6	112.0
S ₃ –C ₄ –P	112.3	114.7	110.7	108.4
C ₂ –P–O	112.8	112.0	114.6	111.9
C ₂ –P–C ₉	105.0	108.8	103.6	105.0
C ₂ –P–C ₁₀	105.0	120.9	103.0	104.1
S ₁ –C ₂ –S ₃ –C ₄	60.0	54.8	67.6	63.5
C ₂ –S ₃ –C ₄ –C ₅	65.2	63.8	66.0	65.3
S ₃ –C ₄ –C ₅ –C ₆	67.2	66.8	63.9	65.1
C ₄ –C ₅ –C ₆ –S ₁	67.3	65.3	66.3	64.8
C ₅ –C ₆ –S ₁ –C ₂	65.2	61.4	67.8	65.5
C ₆ –S ₁ –C ₂ –S ₃	60.0	59.3	67.8	63.9
S ₁ –C ₂ –P–O	66.1	176.4	59.5	176.2
S ₃ –C ₄ –P–O	66.1	41.8	67.5	55.7
C ₄ –S ₃ –C ₂ –P	70.6	87.2	168.0	170.2
C ₆ –S ₁ –C ₂ –P	70.5	87.2	167.2	171.6
S ₁ –C ₂ –P–C ₉	168.8	56.7	174.5	58.3
S ₁ –C ₂ –P–C ₁₀	59.0	53.6	65.8	52.5

^a See Scheme 2 for numbering.

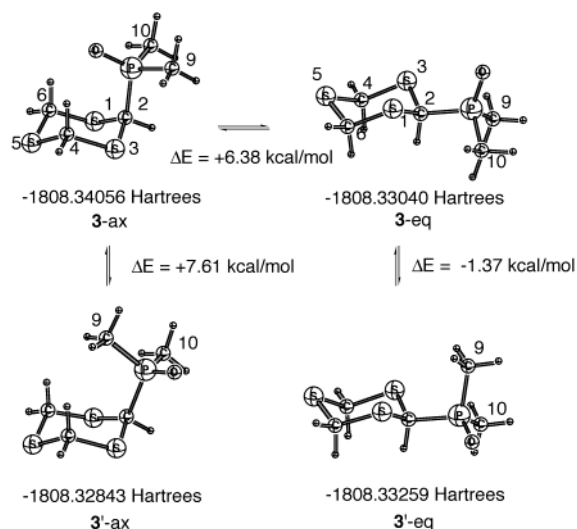
those of 3-ax and 3'-ax ($\Delta E = +7.61$ kcal/mol, Scheme 2). While the former value must reflect the increased steric repulsion in the “methyl inside” relative to the “oxygen inside” rotamers, the much larger energy difference in the latter could arise from an additional stabilization in the rotamer where the phosphoryl function points into the ring. In particular, electrostatic attractive interaction between negatively charged phosphoryl oxygen and the slightly acidic *syn*-axial hydrogens at C(4,6) could help account in part for the experimentally observed increased predominance of axial trithiane 3-ax,^{1b,e,14} as well as for the large calculated energy increase in going from 3-ax (oxygen inside) to 3'-ax (methyl inside) (Scheme 2).

Support for the contribution of hydrogen-bond type stabilizing interactions in 3-ax comes from the analysis of the critical points associated with its electronic topology, as derived from AIM theory.^{8,9} (Table 2 and Figure 3). In contrast with the calculated topology of cyclohexyl derivative 2-ax, in axial trithiane analogue 3-ax it was possible to locate 4 ring critical points, as well as one cage critical point, associated with the presence of a significant interaction between the phosphoryl oxygen and the *syn*-axial hydrogens at C(4,6) (Figure 3). Most important, the calculated electronic density at the *a* and *b* critical points within the P–O–H–C(4,6) bonding path

(14) For literature about intermolecular P–O···H–C hydrogen bonding, see for example: Desiraju, G. R.; Steiner, T. *The Weak Hydrogen Bond in Structural Chemistry and Biology*; Oxford University Press: Oxford, 1999. Green, R. D. *Hydrogen Bonding by C–H Groups*; Macmillan: London, 1974.

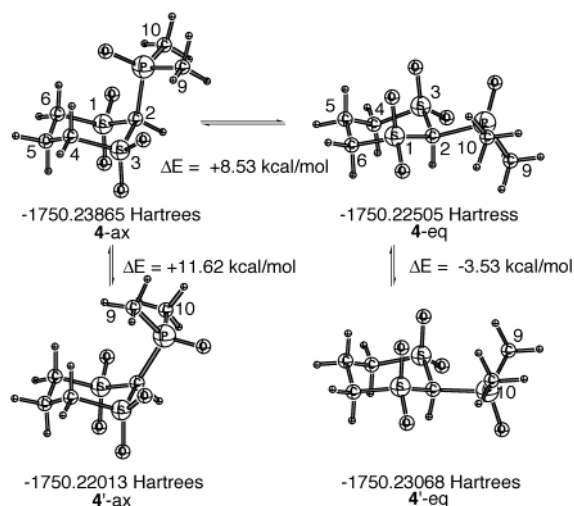
Table 4. Geometry of the Most Relevant Conformers of 2-(Dimethylphosphinoyl)-1,3-dithiane-1,1,3,3-tetraoxide (4) at the B3LYP/6-31G(*d,p*) Level (Distances in Å, Angles in Degrees)^a

	4-ax	4'-ax	4-eq	4'-eq
S ₁ -C ₂	1.871	1.864	1.858	1.846
C ₂ -S ₃	1.871	1.878	1.841	1.846
S ₃ -C ₄	1.816	1.824	1.824	1.822
C ₄ -C ₅	1.531	1.527	1.529	1.530
C ₅ -C ₆	1.531	1.528	1.530	1.530
C ₆ -S ₁	1.816	1.817	1.824	1.822
C ₂ -P	1.895	1.912	1.927	1.935
P-O	1.506	1.494	1.491	1.496
P-C ₉	1.825	1.827	1.822	1.822
P-C ₁₀	1.825	1.822	1.827	1.822
S ₁ -C ₂ -S ₃	110.2	116.7	114.2	112.8
C ₂ -S ₃ -C ₄	102.6	104.8	103.5	102.9
S ₃ -C ₄ -C ₅	112.8	114.4	114.5	113.4
C ₄ -C ₅ -C ₆	113.4	112.8	113.4	113.6
C ₅ -C ₆ -S ₁	112.8	113.1	112.1	113.4
C ₆ -S ₁ -C ₂	102.6	105.2	101.9	102.9
S ₁ -C ₂ -P	113.1	123.0	109.2	114.9
S ₃ -C ₄ -P	113.1	113.8	115.3	114.9
C ₂ -P-O	109.2	108.4	113.2	109.7
C ₂ -P-C ₉	106.4	106.3	106.0	106.4
C ₂ -P-C ₁₀	106.5	107.8	100.0	106.4
S ₁ -C ₂ -S ₃ -C ₄	55.2	46.8	48.8	52.6
C ₂ -S ₃ -C ₄ -C ₅	68.7	54.8	52.7	57.1
S ₃ -C ₄ -C ₅ -C ₆	68.7	68.1	67.0	67.7
C ₄ -C ₅ -C ₆ -S ₁	68.7	57.6	70.9	57.1
C ₅ -C ₆ -S ₁ -C ₂	59.4	48.3	59.8	52.6
C ₆ -S ₁ -C ₂ -S ₃	55.2	46.8	52.1	52.6
S ₁ -C ₂ -P-O	63.1	150.1	28.6	113.3
S ₃ -C ₄ -P-O	63.0	69.7	101.6	113.3
C ₄ -S ₃ -C ₂ -P	72.4	97.9	176.5	173.0
C ₆ -S ₁ -C ₂ -P	72.4	92.6	177.0	173.0
S ₁ -C ₂ -P-C ₉	171.6	85.0	155.4	150.1
S ₁ -C ₂ -P-C ₁₀	62.2	27.2	94.3	11.1

^a See Scheme 3 for numbering.**Scheme 2. Conformational Equilibria of 2-(Dimethylphosphinoyl)-1,3,5-trithiane (3)^a**^a ZPE corrections are not included.

is a substantial $0.012\ e/a_0^3$ (Table 2). Furthermore, the low ellipticity parameter for critical points *a* and *b* in **3-ax** (0.061 for both, Table 2) is indicative of a sizable interaction.¹⁰ (By contrast, $\epsilon = 0.171$ in **2-ax**, Table 2.)

Part C. Conformational Analysis of 2-(Dimethylphosphinoyl)-1,3-dithiane-1,1,3,3-tetraoxide, 4. As summarized in Scheme 3, the axial conformer **4-ax** is estimated to be 5.0 kcal/mol more stable than **4'-eq**. In

**Figure 3.** Critical points in the electron density of **3-ax** calculated at the Becke3LYP/6-31G(*d,p*) level of theory.**Scheme 3. Conformational Equilibria of 2-(Dimethylphosphinoyl)-1,3-dithiane-1,1,3,3-tetraoxide, 4^a**^a ZPE corrections are not included.

4-ax the P-O group points toward the center of the ring, the methyl-inside rotamer **4'-ax** being 11.6 kcal/mol higher in energy. By contrast, in the equatorial conformer **4'-eq** the dimethylphosphinoyl group is substantially eclipsed with the vicinal C(2)-S and C(2)-H bonds, the CH₃-P-C(2)-S torsional angles are 11.2°, and O-P-C(2)-H is 0.0°. Eclipsing in **4'-eq** is necessary in order to minimize the electrostatic repulsion between the phosphoryl and sulfonyl oxygens present in rotamer **4-eq**, which is 3.53 kcal mol⁻¹ higher in energy. Furthermore, conformation **4'-eq** benefits from an attractive S-O...H₃C-P attractive electrostatic interaction.

AIM theory has been successfully applied to study hydrogen bond interactions,^{10,16} permitting a deeper understanding of the various factors responsible for such interactions. Cioslowski¹⁰ has pointed out that for a stable compound in a minimum of its potential surface, there are three kinds of electron density interaction lines: those that describe strong bonds, those that describe weak bonds (with high electronic delocalization), and those that describe repulsive steric interactions. In this regard, the characterization of critical points along such interaction lines allows the establishment of the molec-

(15) For a general discussion of eclipsing in organic molecules, see: Juaristi, E. Stable Eclipsed Conformations. In *Encyclopedia of Computational Chemistry*; Schleyer, P. v. R., Ed.; Wiley: New York, 1998.

(16) Sosa, G. L.; Peruchena, N.; Contreras, R. H.; Castro, E. A. *J. Mol. Struct. (THEOCHEM)* **1997**, 401, 77 and the references therein.



Figure 4. Critical points in the electron density of **4-ax** calculated at the Becke3LYP/6-31G(*d,p*) level of theory.

ular structure as well as the study of unusual chemical bonds since the topological approximation does not show a difference between normal (strong) bonds and those resulting from weak interactions. Nevertheless, the electronic density at a critical point of a weak bond is twenty times less than the density of a critical point in a normal C–H bond.¹⁰

Atomic interaction lines are defined by density trajectories that terminate at nuclei and pass through a critical point of (3, –1) type.

Most relevant to the present study of disulfone **4** are the observed P–O···H(4,6-ax) trajectories indicative of attractive electrostatic interactions between the phosphoryl oxygen and the *syn*-diaxial hydrogens in **4-ax** (critical points *a* and *b* in Figure 4). Two additional trajectories were obtained, associated to attractive electrostatic interactions between the equatorial sulfone oxygens and the proximate hydrogen atoms of the methyl groups joined to the phosphorous atom. These trajectories generated ring critical points (*i*, *h* in Figure 4) that as a whole permitted the satisfaction of the Poincaré–Hopf relationship. For the related critical points to these paths the curvature's principal axes are parallel to the bond trajectory that describes electronic delocalization.

A salient feature in the electron density distribution for **4-ax** (Figure 4) is the O/O trajectory similar to a dihydrogen bond (critical point *l*),¹⁷ whose principal curvature is perpendicular to the bond plane.^{9b} This trajectory that closes a five membered ring also generates a ring critical point. The characteristic ensemble of this molecule is 27, 32, 7, and 1. As can be seen, in every case the Laplacians of the electronic density at the critical points are positive; this is indicative of weaker interactions or bonds with high ionic character. The weak bonds trajectories are larger than their geometric distance, which agrees with the proposal that the weak interactions are curved in the space as could be seen in previous reported cases.¹⁰

In the equatorial conformer the topology is very simple (Figure 5). Only bond paths between the equatorial sulfonyl oxygens and the *P*-methyl group hydrogen atoms (points *a* and *b* in Figure 5) are evident. The associated ring critical points to the weak interactions and those related to the 1,3-dithiane ring were also determined. There is no relevant repulsive interaction between the *syn*-diaxial oxygen atoms, nor between sulfonyl oxygens

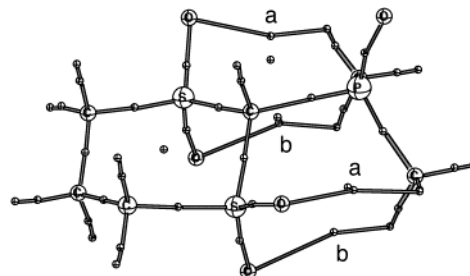
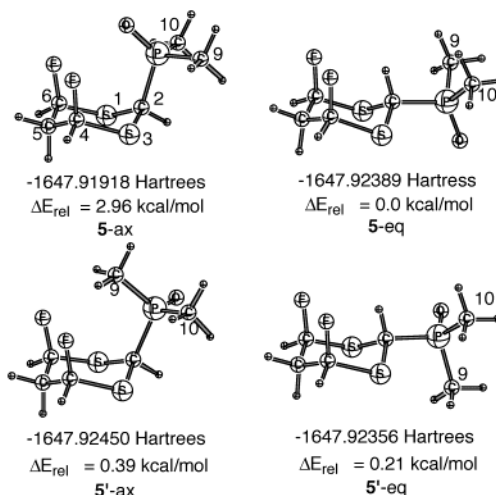


Figure 5. Critical points in the electron density of **4-eq** calculated at the Becke3LYP/6-31G(*d,p*) level of theory.

Scheme 4. Relevant Conformers of 4,6-Difluoro-2-(dimethylphosphinoyl)-1,3-dithiane Calculated at the Becke3LYP/6-31G(*d,p*) Level of Theory^a



^a ZPE corrections are not included.

and the phosphinoyl oxygen atom. Thus arguments based on dominant electrostatic repulsion in **4'-eq** may be discarded.

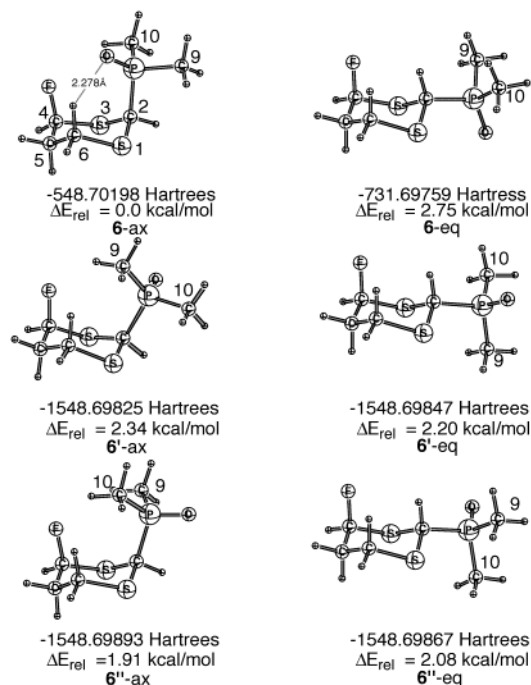
To know whether electron density remains unaltered at higher levels of theory, calculations at the Becke3LYP/6-311++G(2*d*,2*p*)/Becke3LYP/6-31G(*d,p*) were performed for **4-ax** and **4'-eq**. Properties of critical points of **4-ax** are very similar to those described in Table 2, giving evidence of low sensibility of these properties to basis set effects. The difference in energy between both conformers is estimated as 5.1 kcal/mol (versus 5.0 kcal/mol at the Becke3LYP/6-31G(*d,p*) level).

Part D. Conformational Analysis of *r*2,*c*4,*c*6-4,6-Difluoro-2-(dimethylphosphinoyl)- (5) and *r*2,*c*4-2-(Dimethylphosphinoyl)-4-fluoro-1,3-dithiane (6). Schemes 4 and 5 include the total and relative energies of the four low-energy conformers of the difluorinated compound **5** and the six conformers of the monofluorinated derivative **6**, respectively. For comparison purposes, only those chair arrangements with *syn*-diaxial fluorine atoms were considered. Nevertheless, the final geometry corresponds to a fully relaxed structure.

Conformer **5-ax** is now the least stable of all minima, by practically 3 kcal/mol. The remaining conformers have similar energy and could coexist in solution. Because of the strong repulsion between the phosphoryl oxygen and the fluorine atoms, the O–P–C bond angle is 117.5°, to be compared with the observed O–P–C bond angle of 113.3° in **3-ax**.

(17) Alkorta, I.; Rozas, I.; Elguero, J. *Chem. Soc. Rev.* **1998**, 27, 163.

Scheme 5. Relevant Conformers of 4-Fluoro-2-(dimethylphosphinoyl)-1,3-dithiane^a



^a ZPE corrections are not included.

Interestingly, in the monofluorinated derivative, **6-ax** is now the most stable conformer. In this arrangement the phosphoryl oxygen points toward the *syn*-axial hydrogen atom, H(6-ax). A bond critical point and a bond path were determined, as well as the associated critical points that allow to satisfy the Poncare-Hopf relationship. At this bond critical point the ρ value is 0.015 e/a_0^3 , $\nabla^2\rho$ is 0.047 , ϵ is 0.055 , and the total bond length is 4.342 au , 0.037 au larger than the geometric distance (4.305 au) between the bonded nuclei.

In terms of density at the bond critical point, this is the strongest interaction described in Table 2, giving evidence that a bifurcated interaction contributes to a better stabilization relative to a single O–H bond. Indeed, in eqs 3 and 4 a bifurcated hydrogen bond is preferred over a single hydrogen bond.

Summary and Conclusions

Ab initio calculations (B3LYP/6-31G(*d,p*)) seem to reproduce the experimentally determined axial predominance of 2-(diphenylphosphinoyl)-1,3,5-trithiane, as well as the equatorial preference of (diphenylphosphinoyl)-cyclohexane. Calculations lead to the prediction that the conformational equilibrium in 2-(dimethylphosphinoyl)-1,3-dithiane-1,1,3,3-tetraoxide (**4**) should favor the axial isomer. This result is particularly relevant since the lack of sulfur lone pairs precludes $n_{\text{S}} \rightarrow \sigma^*_{\text{C-P}}$ hyperconjugation that could account for stereoelectronic stabilization in the (*gauche* = axial) S–C–P segments.

The destabilization of the difluorinated derivative **5-ax**, and the bond path described for **6-ax**, establishes the electrostatic nature of the interaction. The C–H–O–P bond trajectories were described. The density at the bond critical point reflects the strength of the interaction, that could be a dominant contribution to the observed conformational preference.

Topological analysis of the electronic density in the relevant conformers of axial and equatorial **2–6** was carried out within AIM's theoretical framework. The equatorial preference of **2-eq** is then ascribed to normal steric repulsion in the axial phosphorylated cyclohexane. By contrast, examination of the properties of critical points in bond trajectories associated to **3-ax** and **4-ax** lead to the conclusion that hydrogen-bonding of nonconventional type contributes to the axial stability of the phosphorylated trithiane, **3**, and 1,3-dithiane sulfone, **4**.

Acknowledgment. The authors deeply express their gratitude to the Dirección General de Servicios de Cómputo Académico (UNAM) for supercomputer CPU time and to CONACYT, Grants 32420-E and L0006-E, and DGAPA IN107597. G.M. and A.R. are grateful to CONACYT for financial support.

Supporting Information Available: The Cartesian coordinates with the computed total energies (Hartrees) for *axial* and *equatorial* conformers of compound **4-ax** and **4-eq**. This material is available free of charge via the Internet at <http://pubs.acs.org>.

JO001505A